HEFAT2014
10th International Conference on Heat Transfer, Fluid Mechanics and Thermodynamics
14 – 16 July 2014
Orlando, Florida

MHD MIXED CONVECTION IN MICROPOLAR FLUID WITH CROSS DIFFUSION EFFECTS

Srinivasacharya D.* and Upendar M.
*Author for correspondence
Department of Mathematics,
National Institute of Technology Warangal,
Andhra Pradesh, 506004,
India.
E-mail: dsc@nitw.ac.in, dsrinivasacharya@yahoo.com

ABSTRACT

This paper analyzes cross diffusion effects on the steady, mixed convection heat and mass transfer along a semi-infinite vertical plate embedded in a micropolar fluid in the presence of traverse magnetic field. The governing nonlinear partial differential equations and their associated boundary conditions are transformed into a system of coupled nonlinear ordinary differential equations using a special form of Lie group transformations, namely, the scaling group of transformations and then solved numerically using the implicit finite difference method. The non dimensional velocity, microrotation, temperature and concentration along with the non dimensional rate of heat and mass transfer at the plate are presented graphically for different values of coupling number, magnetic parameter (M), mixed convection parameter (R_i), Soret number (S_r) and Dufour number (D_f). In addition, the skin-friction coefficient and the wall couple stress are shown in a tabular form.

NOMENCLATURE

B	Buoyancy parameter $= (\beta_C \Delta C)/(\beta_T \Delta T)$
B_0	Magnetic field coefficient
C	Concentration of the field
C_p	Specific heat at constant pressure
C_s	Concentration susceptibility
$\bar{C}_\infty$	Free stream concentration
C_f	Skin-friction coefficient
D	Mass diffusivity
D_f	Dufour number $(= \frac{D K_T \Delta C}{C_s C_p \nu \Delta T})$
f	Dimensionless stream function
g	Dimensionless microrotation
g^*	Acceleration due to gravity
Gr	Grashof number $(= g^* \beta_T \Delta T L^3 / \nu^2)$
j	Dimensional Micro-inertia density
k	Thermal conductivity
k_1	Mean absorption coefficient
k_T	Thermal diffusion ratio
L	Characteristic length
m_w	Wall couple stress
M	Non-dimensional magnetic parameter $= (\sigma B_0^2 L^2)/(\mu \mathrm{Re})$
M_w	Non-dimensional couple stress on the wall
N	Coupling number $(= \frac{\kappa}{\kappa + \mu})$
N_u	Dimensionless Nusselt number
Pr	Prandtl number, non-dimensional $= \frac{\nu}{\alpha}$
$q_w(\bar{x})$	Heat flux
$q_m(\bar{x})$	Mass flux
Re	Reynolds number, dimensionless
Ri	Mixed convection parameter $(= \frac{Gr}{\mathrm{Re}^2})$
s	Dimensionless concentration
Sc	Schmidt number, non-dimensional $= \frac{\nu}{D}$
Sh	Sherwood number
S_r	Soret number $(= \frac{D K_T \Delta T}{T_m \nu \Delta C})$
$\bar{T}$	Temperature
T_m	Mean fluid temperature
$\bar{T}_\infty$	Free stream temperature
$U(\bar{x})$	Free stream velocity
$\bar{u}, \bar{v}$	Velocity components in the $\bar{x}$- and $\bar{y}$-directions respectively.
$\bar{x}$, $\bar{y}$	Cartesian coordinates along the plate and normal to it
$\hat{x}$, $\hat{y}$	Lie Group transformations of co-ordinate axes

Greek symbols

α	Thermal diffusivity
α_i's	Lie Group transformation parameters *(i = 1 to 6)*
β_T	Coefficient of thermal expansion
β_C	Coefficient of solutal expansion
γ	Spin-gradient viscosity
η	Non-dimensional similarity variable
θ	Dimensionless temperature
$\hat{\theta}$	Lie Group transformation of temperature

ϑ Non-dimensional micro-inertia density ($= \frac{L^2}{j\,\mathrm{Re}}$)

κ Vortex viscosity

λ Spin-gradient viscosity ($= \frac{\gamma}{j\,\rho\,\nu}$)

μ Viscosity of the fluid

ν Kinematic viscosity

ρ Density of the base fluid

σ Electrical conductivity

τ_w Wall shear stress

ϕ Dimensionless concentration

$\hat{\phi}$ Lie Group transformation

ψ Stream function

$\hat{\psi}$ Lie Group transformation of stream function

$\bar{\omega}$ Microrotation component

$\hat{\omega}$ Lie Group transformation of micromotion component

INTRODUCTION

Mixed convection flows are of great interest because of their various engineering, scientific, and industrial applications in heat and mass transfer. Mixed convection of heat and mass transfer occurs simultaneously in the fields of design of chemical processing equipment, formation and dispersion of fog, distributions of temperature, moisture over agricultural fields, groves of fruit trees, and damage of crops due to freezing and pollution of the environment. Extensive studies of mixed convection heat and mass transfer of a non-isothermal vertical surface under boundary layer approximation have been undertaken by several authors. The majority of these studies dealt with the traditional Newtonian fluids. It is well known that most fluids which are encountered in chemical and allied processing applications do not satisfy the classical Newton's law and are accordingly known as non-Newtonian fluids. Due to the important applications of non-Newtonian fluids in biology, physiology, technology, and industry, considerable efforts have been directed towards the analysis and understanding of such fluids. A number of mathematical models have been proposed to explain the rheological behaviour of non-Newtonian fluids. Among these, the fluid model introduced by Eringen [1] exhibits some microscopic effects arising from the local structure and micro motion of the fluid elements. Further, they can sustain couple stresses and include classical Newtonian fluid as a special case. The model of micropolar fluid represents fluids consisting of rigid, randomly oriented (or spherical) particles suspended in a viscous medium where the deformation of the particles is ignored. Micropolar fluids have been shown to accurately simulate the flow characteristics of polymeric additives, geomorphologic sediments, colloidal suspensions, haematological suspensions, liquid crystals, lubricants etc. The heat and mass transfer in micropolar fluids is also important in the context of chemical engineering, aerospace engineering and also industrial manufacturing processes. The problem of free convection, heat and mass transfer in the boundary layer flow along a vertical surface submerged in a micropolar fluid has been studied by several investigators.

In recent years, several simple boundary layer flow problems have received new attention within the more general context of magneto hydrodynamics (MHD). Several investigators have extended many of the available boundary layer solutions to include the effects of magnetic fields for those cases when the fluid is electrically conducting. The study of magneto-hydrodynamic flow for an electrically conducting fluid past a heated surface has important applications in many engineering problems such as plasma studies, petroleum industries, MHD power generators, cooling of nuclear reactors, the boundary layer control in aerodynamics, and crystal growth. In addition, there has been a renewed interest in studying MHD flow and heat transfer in porous media due to the effect of magnetic fields on flow control and on the performance of many systems using electrically conducting fluids. The problem of MHD mixed convection heat and mass transfer in the boundary layer flow along a vertical surface submerged in a micropolar fluid has been studied by several investigators. Seddeek [2] investigated the analytical solution for the effect of radiation on flow of a magneto-micropolar fluid past a continuously moving plate with suction and blowing. Mahmoud [3] analyzed the effects of slip and heat generation/absorption on MHD mixed convection flow of a micropolar fluid over a heated stretching surface. Tzirtzilakis et al. [4] studied the action of a localized magnetic field on forced and free convective boundary layer flow of a magnetic fluid over a semi-infinite vertical plate. Hayat [5] studied the effects of heat and mass transfer on the mixed convection flow of a MHD micropolar fluid bounded by a stretching surface using Homotopy analysis method. Das [6] considered the effects of partial slip on steady boundary layer stagnation point flow of an electrically conducting micropolar fluid impinging normally towards a shrinking sheet in the presence of a uniform transverse magnetic field.

In most of the studies related to heat and mass transfer process, Soret (mass fluxes can also be created by temperature gradients) and Dufour (energy flux caused by a concentration gradient) effects were neglected on the basis that they are of a smaller order of magnitude than the effects described by Fourier's and Fick's laws. But these effects are considered as second order phenomena and may become significant in areas such as hydrology, petrology, geosciences, etc. The Soret effect, for instance, has been utilized for isotope separation and in mixture between gases with very light molecular weight and of medium molecular weight. The Dufour effect was recently found to be of order of considerable magnitude so that it cannot be neglected [7]. Alam and Rahman [8] have investigated the Dufour and Soret effects on mixed convection flow past a vertical porous flat plate with variable suction. Chamkha [9] has focused on the numerical modelling of the effects of Soret, Dufour and radiation on heat and mass transfer by MHD mixed convection from a semi-infinite, isothermal, vertical and permeable surface immersed in a uniform porous medium. Rawat and Bhargava [10] presented a mathematical model for the steady thermal convection heat and mass transfer in a micropolar fluid saturated Darcian porous medium in the presence of significant Dufour and Soret effects and viscous heating. Srinivasacharya and RamReddy [11] studied Soret and Dufour effects on the mixed convection from a semi-infinite vertical plate embedded in a stable micropolar fluid with uniform and constant heat and mass flux conditions.

The Lie group analysis, also called symmetry analysis, has been developed by *Sophius Lie* to find point transformations

which map a given differential equation to itself. This method reduces the number of independent variables by one and consequently the governing partial differential equations are transformed into ordinary differential equations with the associated boundary conditions. This method has drawn the attention of several researchers [12-18] to analyze various convective phenomena subject to various flow configurations arising in fluid mechanics, aerodynamics, plasma physics, meteorology and some branches of engineering.

Inspired by the investigations mentioned above, the aim of this paper is to consider the effects of transverse magnetic field, Soret and Dufour effects on the mixed convection heat and mass transfer along a vertical plate with variable heat and mass flux conditions embedded in a micropolar fluid. The governing nonlinear partial differential equations of boundary layer problem are transformed into a system of coupled nonlinear ordinary differential equations using a scaling group of transformations. The Keller-box method given in Cebeci and Bradshaw [19] is employed to solve this nonlinear system of equations. The results thus obtained are compared that of the existing results and found to be in good agreement.

MATHEMATICAL FORMULATION

Consider a steady, laminar, incompressible, two-dimensional mixed convective heat and mass transfer along a semi infinite vertical plate embedded in a free stream of electrically conducting micropolar fluid with velocity $U(\bar{x})$, temperature $\bar{T}_\infty$ and concentration $\bar{C}_\infty$. Choose the co-ordinate system such that $\bar{x}$ axis is along the vertical plate and $\bar{y}$ axis normal to the plate. The plate is maintained with variable heat flux $q_w(\bar{x})$ and mass flux $q_m(\bar{x})$. A uniform magnetic field of magnitude B_0 is applied normal to the plate. The magnetic Reynolds number is assumed to be small so that the induced magnetic field can be neglected in comparison with the applied magnetic field. The Boussinesq approximation is invoked for the fluid properties to relate density changes, and to couple in this way the temperature and concentration fields, $\rho = \rho_\infty\left(1-\beta_T\left(T-T_\infty\right)-\beta_C\left(C-C_\infty\right)\right)$ to the flow field. In addition, the Soret and Dufour effects are considered.

Using the Boussinesq and boundary layer approximations, the governing equations for the micropolar fluid are given by

$$\frac{\partial \bar{u}}{\partial \bar{x}}+\frac{\partial \bar{v}}{\partial \bar{y}}=0 \tag{1}$$

$$\rho\left(\bar{u}\frac{\partial \bar{u}}{\partial \bar{x}}+\bar{v}\frac{\partial \bar{u}}{\partial \bar{y}}\right)=\rho U(\bar{x})\frac{dU(\bar{x})}{d\bar{x}}+\left(\mu+\kappa\right)\frac{\partial^2 \bar{u}}{\partial \bar{y}^2}+$$
$$\kappa\frac{\partial \bar{\omega}}{\partial \bar{y}}+\rho g^*\left(\beta_T\left(\bar{T}-\bar{T}_\infty\right)+\beta_C\left(\bar{C}-\bar{C}_\infty\right)\right)+ \tag{2}$$
$$\sigma B_0^2\left(U(\bar{x})-\bar{u}\right)$$

$$\rho j\left(\bar{u}\frac{\partial \bar{\omega}}{\partial \bar{x}}+\bar{v}\frac{\partial \bar{\omega}}{\partial \bar{y}}\right)=\gamma\frac{\partial^2 \bar{\omega}}{\partial \bar{y}^2}-\kappa\left(2\bar{\omega}+\frac{\partial \bar{u}}{\partial \bar{y}}\right) \tag{3}$$

$$\bar{u}\frac{\partial \bar{T}}{\partial \bar{x}}+\bar{v}\frac{\partial \bar{T}}{\partial \bar{y}}=\alpha\frac{\partial^2 \bar{T}}{\partial \bar{y}^2}+\frac{DK_T}{C_sC_p}\frac{\partial^2 \bar{C}}{\partial \bar{y}^2} \tag{4}$$

$$\bar{u}\frac{\partial \bar{C}}{\partial \bar{x}}+\bar{v}\frac{\partial \bar{C}}{\partial \bar{y}}=D\frac{\partial^2 \bar{C}}{\partial \bar{y}^2}+\frac{DK_T}{T_m}\frac{\partial^2 \bar{T}}{\partial \bar{y}^2} \tag{5}$$

where $\bar{u}$ and $\bar{v}$ are the components of velocity along $\bar{x}$ - and $\bar{y}$ - directions respectively, $\bar{\omega}$ is the component of microrotation whose direction of rotation lies normal to the $\bar{x}\bar{y}$ - plane, g^* is the gravitational acceleration, $\bar{T}$ is the temperature, $\bar{C}$ is the concentration, β_T is the coefficient of thermal expansions, β_c is the coefficient of solutal expansion. C_p is the specific heat capacity, B_0 is the coefficient of the magnetic field, μ is the dynamic coefficient of viscosity of the fluid, κ is the vertex viscosity, j is the micro-inertia density, γ is the spin gradient viscosity, σ is the magnetic permeability of the fluid, υ is the kinematic viscosity of the fluid, α is the thermal diffusivity, D is the molecular diffusivity, K_T is the thermal diffusion ratio, C_s is the concentration susceptibility, T_m is the mean fluid temperature. Equations (1) - (3) represent the conservation of mass, conservation of momentum and conservation of angular momentum, respectively. The last term of the Equation (2) stands for the Lorenz force term. The term $\left(\sigma B_0^2/\rho\right)U(\bar{x})$ represents the imposed pressure force in the inviscid region of the conducting fluid and $\left(\sigma B_0^2/\rho\right)u$ represents the Lorentz force imposed by a transverse magnetic field to an electrically conducting fluid. The Equations (4) and (5) denote energy and concentration equations respectively.

The boundary conditions for the velocity, microrotation, temperature and concentration distributions for the present problem can be considered as:

$$\bar{u}=0,\ \bar{v}=0,\ \bar{\omega}=0,\ -k\frac{\partial \bar{T}}{\partial \bar{y}}=q_w\left(\bar{x}\right),\ -D\frac{\partial \bar{C}}{\partial \bar{y}}=q_m\left(\bar{x}\right) \quad \text{at } \bar{y}=0 \tag{6a}$$

$$\bar{u}\to U(\bar{x}),\ \bar{\omega}=0,\ \bar{T}\to\bar{T}_\infty,\ \bar{C}\to\bar{C}_\infty \text{ as } \bar{y}\to\infty \tag{6b}$$

The boundary condition $\bar{\omega}=0$ in Eq. (6a), represents the case of concentrated particle flows in which the microelements close to the wall are not able to rotate, due to the no-slip condition.

Introduce the following non – dimensional variables

$$\left.\begin{aligned} &x=\frac{\bar{x}}{L},\ y=\frac{\bar{y}\sqrt{\mathrm{Re}}}{L},\ u=\frac{\bar{u}}{U_\infty},\ v=\frac{\bar{v}\sqrt{\mathrm{Re}}}{U_\infty},\ \mathrm{Re}=\frac{U_\infty L}{\nu},\\ &\omega=\frac{\bar{\omega}L}{U_\infty\sqrt{\mathrm{Re}}},\ U(x)=U_\infty x\\ &\bar{T}=\bar{T}_\infty+\frac{q_w(\bar{x})}{Lk\sqrt{\mathrm{Re}}}\theta,\ \ \frac{q_w(\bar{x})}{k}=\Delta T\,\bar{x}\sqrt{\mathrm{Re}},\\ &\bar{C}=\bar{C}_\infty+\frac{q_m(\bar{x})}{LD\sqrt{\mathrm{Re}}}\varphi,\ \ \frac{q_m(\bar{x})}{D}=\Delta C\,\bar{x}\sqrt{\mathrm{Re}} \end{aligned}\right\} \tag{7}$$

and the stream function ψ in view of (1) through $u=\frac{\partial \psi}{\partial y}$, $v=-\frac{\partial \psi}{\partial x}$ in to Eqs. (2) – (5), we get

$$\frac{\partial \psi}{\partial y}\frac{\partial^2 \psi}{\partial x \partial y}-\frac{\partial \psi}{\partial x}\frac{\partial^2 \psi}{\partial y^2}=x+\frac{1}{1-N}\frac{\partial^3 \psi}{\partial y^3}+. \\ \left(\frac{N}{1-N}\right)\frac{\partial \omega}{\partial y}+R_i x(\theta+B\varphi)+M\left(x-\frac{\partial \psi}{\partial y}\right) \tag{8}$$

$$\frac{\partial \psi}{\partial y}\frac{\partial \omega}{\partial x}-\frac{\partial \psi}{\partial x}\frac{\partial \omega}{\partial y}=\lambda\frac{\partial^2 \omega}{\partial y^2}-\frac{N}{1-N}\vartheta\left(2\omega+\frac{\partial^2 \psi}{\partial y^2}\right) \tag{9}$$

$$x\frac{\partial \psi}{\partial y}\frac{\partial \theta}{\partial x}-x\frac{\partial \psi}{\partial x}\frac{\partial \theta}{\partial y}+\theta\frac{\partial \psi}{\partial y}=\frac{x}{\Pr}\frac{\partial^2 \theta}{\partial y^2}+x D_f\frac{\partial^2 \varphi}{\partial y^2} \tag{10}$$

$$x\frac{\partial \psi}{\partial y}\frac{\partial \varphi}{\partial x}-x\frac{\partial \psi}{\partial x}\frac{\partial \varphi}{\partial y}+\varphi\frac{\partial \psi}{\partial y}=\frac{x}{Sc}\frac{\partial^2 \varphi}{\partial y^2}+x S_r\frac{\partial^2 \theta}{\partial y^2} \tag{11}$$

The transformed boundary conditions are

$$\frac{\partial \psi}{\partial y}=0,\ \frac{\partial \psi}{\partial x}=0,\ \omega=0,\ \frac{\partial \theta}{\partial y}=-1,\ \frac{\partial \varphi}{\partial y}=-1,\ \text{at } y=0 \tag{12a}$$

$$\frac{\partial \psi}{\partial y}\to x,\quad \omega\to 0,\quad \theta\to 0,\quad \varphi\to 0 \qquad \text{as } y\to\infty \tag{12b}$$

where $N=\frac{\kappa}{\kappa+\mu},(0\le N<1)$ is the Coupling number, $R_i=\frac{Gr}{\mathrm{Re}^2}$ is the mixed convection parameter, $Gr=g^*\beta_T\Delta T L^3/\nu^2$, is the Grashof number, *Re* is the Reynolds number, $M=\left(\sigma B_0^2 L^2\right)/\left(\mu\,\mathrm{Re}\right)$ is the magnetic field parameter, $\lambda=\gamma/(j\rho\nu)$ is the spin-gradient viscosity, $\vartheta=L^2/(j\,\mathrm{Re})$ is the micro-inertia density, $D_f=\left(D K_T\,\Delta C\right)/\left(C_s C_p \nu\Delta T\right)$ is the Dufour number and $S_r=\left(D K_T\,\Delta T\right)/\left(T_m \nu\,\Delta C\right)$ is the Soret number.

SIMILARITY SOLUTIONS VIA LIE GROUP ANALYSIS

We now introduce the one-parameter scaling group of transformations which is a simplified form of Lie group transformation Γ:

$$\left.\begin{aligned}&\hat{x}=xe^{\varepsilon\alpha_1},\quad \hat{y}=ye^{\varepsilon\alpha_2},\quad \hat{\psi}=\psi e^{\varepsilon\alpha_3},\\ &\hat{\omega}=\omega e^{\varepsilon\alpha_4},\ \hat{\theta}=\theta e^{\varepsilon\alpha_5},\ \hat{\varphi}=\varphi e^{\varepsilon\alpha_6}\end{aligned}\right\} \tag{13}$$

where $\alpha_1,\ \alpha_2,\ \alpha_3,\ \alpha_4,\ \alpha_5,\ \alpha_6$ are transformation parameters and ε is a small parameter. This scaling group of transformations transform co-ordinates (x, y, $\psi,\omega,\theta,\varphi$) to $\left(\hat{x},\ \hat{y},\ \hat{\psi},\ \hat{\omega},\ \hat{\theta},\ \hat{\varphi}\right)$. Equations (8) to (11) and boundary conditions Eq. (12) are invariant under the point transformations (13).

Substituting the transformations (13) into Eqs. (8) – (11) and boundary conditions (12), we get

$$\left.\begin{aligned}&e^{\varepsilon(\alpha_1+2\alpha_2-2\alpha_3)}\left(\frac{\partial \hat{\psi}}{\partial \hat{y}}\frac{\partial^2 \hat{\psi}}{\partial \hat{x}\partial \hat{y}}-\frac{\partial \hat{\psi}}{\partial \hat{x}}\frac{\partial^2 \hat{\psi}}{\partial \hat{y}^2}\right)=e^{-\varepsilon\alpha_1}\hat{x}+\\ &e^{\varepsilon(3\alpha_2-\alpha_3)}\frac{1}{1-N}\frac{\partial^3 \hat{\psi}}{\partial \hat{y}^3}+e^{\varepsilon(\alpha_2-\alpha_4)}\left(\frac{N}{1-N}\right)\frac{\partial \hat{\omega}}{\partial \hat{y}}+R_i\hat{x}\\ &\left(e^{\varepsilon(-\alpha_1-\alpha_5)}\hat{\theta}+Be^{\varepsilon(-\alpha_1-\alpha_6)}\hat{\varphi}\right)+M\left(e^{-\varepsilon\alpha_1}\hat{x}-e^{\varepsilon(\alpha_2-\alpha_3)}\frac{\partial \hat{\psi}}{\partial \hat{y}}\right)\end{aligned}\right\} \tag{14}$$

$$e^{\varepsilon(\alpha_1+\alpha_2-\alpha_3-\alpha_4)}\left(\frac{\partial \hat{\psi}}{\partial \hat{y}}\frac{\partial \hat{\omega}}{\partial \hat{x}}-\frac{\partial \hat{\psi}}{\partial \hat{x}}\frac{\partial \hat{\omega}}{\partial \hat{y}}\right)=\lambda e^{\varepsilon(2\alpha_2-\alpha_4)}\frac{\partial^2 \hat{\omega}}{\partial \hat{y}^2} \\ -\frac{N}{1-N}\vartheta\left(2e^{-\varepsilon\alpha_4}\hat{\omega}+e^{\varepsilon(2\alpha_2-\alpha_3)}\frac{\partial^2 \hat{\psi}}{\partial \hat{y}^2}\right) \tag{15}$$

$$e^{\varepsilon(\alpha_2-\alpha_3-\alpha_5)}\left(\hat{x}\frac{\partial \hat{\psi}}{\partial \hat{y}}\frac{\partial \hat{\theta}}{\partial \hat{x}}-\hat{x}\frac{\partial \hat{\psi}}{\partial \hat{x}}\frac{\partial \hat{\theta}}{\partial \hat{y}}\right)+e^{\varepsilon(\alpha_2-\alpha_3-\alpha_5)} \\ \hat{\theta}\frac{\partial \hat{\psi}}{\partial \hat{y}}=\frac{e^{\varepsilon(-\alpha_1+2\alpha_2-\alpha_5)}\hat{x}}{\Pr}\frac{\partial^2 \hat{\theta}}{\partial \hat{y}^2}+\hat{x}D_f e^{\varepsilon(-\alpha_1+2\alpha_2-\alpha_6)}\frac{\partial^2 \hat{\varphi}}{\partial \hat{y}^2} \tag{16}$$

$$e^{\varepsilon(\alpha_2-\alpha_3-\alpha_6)}\left(\hat{x}\frac{\partial \hat{\psi}}{\partial \hat{y}}\frac{\partial \hat{\varphi}}{\partial \hat{x}}-\hat{x}\frac{\partial \hat{\psi}}{\partial \hat{x}}\frac{\partial \hat{\varphi}}{\partial \hat{y}}\right)+e^{\varepsilon(\alpha_2-\alpha_3-\alpha_6)} \\ \hat{\varphi}\frac{\partial \hat{\psi}}{\partial \hat{y}}=\frac{e^{\varepsilon(-\alpha_1+2\alpha_2-\alpha_6)}\hat{x}}{Sc}\frac{\partial^2 \hat{\varphi}}{\partial \hat{y}^2}+\hat{x}D_f e^{\varepsilon(-\alpha_1+2\alpha_2-\alpha_6)}\frac{\partial^2 \hat{\theta}}{\partial \hat{y}^2} \tag{17}$$

The boundary conditions (12) becomes

$$\frac{\partial \hat{\psi}}{\partial \hat{y}}=0,\ \frac{\partial \hat{\psi}}{\partial \hat{x}}=0,\ \hat{\omega}=0,\ \frac{\partial \hat{\theta}}{\partial \hat{y}}e^{\varepsilon(\alpha_2-\alpha_5)}=-1,\ \frac{\partial \hat{\varphi}}{\partial \hat{y}}e^{\varepsilon(\alpha_2-\alpha_6)}=-1, \\ \text{at } \hat{y}e^{-\varepsilon\alpha_2}=0 \tag{18a}$$

$$e^{-\varepsilon(\alpha_2-\alpha_3)}\frac{\partial \psi}{\partial y}\to e^{-\varepsilon\alpha_1}\hat{x},\quad \hat{\omega}\to 0,\quad \hat{\theta}\to 0,\quad \hat{\varphi}\to 0 \\ \text{as } \hat{y}e^{-\varepsilon\alpha_2}\to\infty \tag{18b}$$

Since the group transformations (13) keep the system invariant, we then have following relationships among the parameters

$$\left.\begin{aligned}&\alpha_1+2\alpha_2-2\alpha_3=-\alpha_1=3\alpha_2-\alpha_3=\alpha_2-\alpha_4=\\ &-\alpha_1-\alpha_5=-\alpha_1-\alpha_6=-\alpha_1=\alpha_2-\alpha_3\\ &\alpha_1+\alpha_2-\alpha_3-\alpha_4=2\alpha_2-\alpha_4=-\alpha_4=2\alpha_2-\alpha_3\\ &\alpha_2-\alpha_3-\alpha_5=\alpha_1+2\alpha_2-\alpha_5=-\alpha_1+2\alpha_2-\alpha_6\\ &\alpha_2-\alpha_3-\alpha_6=\alpha_1+2\alpha_2-\alpha_6=-\alpha_1+2\alpha_2-\alpha_5\end{aligned}\right\} \tag{19}$$

Solving the linear system Eq. (19), we have the following relationship among the exponents

$$\alpha_1=\alpha_3=\alpha_4 \text{ and } \alpha_2=\alpha_5=\alpha_6=0 \tag{20}$$

Hence, the set of transformations Γ reduces to

$$\left.\begin{aligned}&\hat{x}=xe^{\varepsilon\alpha_1},\quad \hat{y}=y,\quad \hat{\psi}=\psi e^{\varepsilon\alpha_1},\\ &\hat{\omega}=\omega e^{\varepsilon\alpha_1},\ \hat{\theta}=\theta,\quad \hat{\varphi}=\varphi\end{aligned}\right\} \tag{21}$$

Expanding the Lie Group of point transformations in one parameter using the Taylor's series in powers of ε, keeping the terms up to the first degree (neglecting higher powers of ε), we get

$$\left.\begin{aligned}&\hat{x}-x=x\varepsilon\alpha_1,\ \hat{y}-y=0,\ \hat{\psi}-\psi=\psi\varepsilon\alpha_1,\\ &\hat{\theta}-\theta=0,\ \hat{\varphi}-\varphi=0\end{aligned}\right\} \tag{22}$$

The corresponding characteristic equations of (22) are given by

$$\frac{dx}{\varepsilon\alpha_1}=\frac{dy}{0}=\frac{d\psi}{\varepsilon\alpha_1}=\frac{d\omega}{\varepsilon\alpha_1}=\frac{d\theta}{0}=\frac{d\varphi}{0} \tag{23}$$

Solving the above characteristic equations, we have following similarity transformations

$$\hat{y}=\eta,\ \hat{\psi}=\hat{x}f(\eta),\ \hat{\omega}=\hat{x}g(\eta),\ \hat{\theta}=\theta(\eta),\ \hat{\varphi}=\varphi(\eta) \tag{24}$$

Substitute the Eq. (24) into Eqs. (14) to (17), we get

$$\left(\frac{1}{1-N}\right) f'''+ ff''+\left(\frac{N}{1-N}\right) g'-\left(f'\right)^2 + R_i\left(\theta+B\varphi\right)+\left(1-f'\right)M+1=0 \tag{25}$$

$$\lambda g''-\left(\frac{N}{1-N}\right)\vartheta\left(2g+f''\right)-f'g+fg'=0 \tag{26}$$

$$\frac{1}{\Pr}\theta''+f\theta'-f'\theta+D_f\varphi''=0 \tag{27}$$

$$\frac{1}{Sc}\varphi''+f\varphi'-f'\varphi+s_r\theta''=0 \tag{28}$$

$$f(0)=0,\ f'(0)=0,\ g(0)=0,\ \theta'(0)=-1,\ \varphi'(0)=-1 \text{ at } \eta=0 \tag{29a}$$

$$f'(\infty)\to 1,\ g(\infty)\to 0,\ \theta(\infty)\to 0,\ \varphi(\infty)\to 0 \text{ at } \eta\to\infty \tag{29b}$$

The wall shear stress and the wall couple stress are $\tau_w=\left[\left(\mu+\kappa\right)\frac{\partial\bar{u}}{\partial\bar{y}}+\kappa\bar{\omega}\right]_{\bar{y}=0}$, $m_w=\gamma\left[\frac{\partial\bar{\omega}}{\partial\bar{y}}\right]_{\bar{y}=0}$. The dimensionless wall shear stress $C_f=\frac{2\tau_w}{\rho U_\infty^{\,2}}$, wall couple stress $M_w=\frac{m_w}{L\rho U_\infty^{\,2}}$, are given by $C_f\sqrt{\mathrm{Re}}=\left(\frac{2}{1-N}\right)f''(0)x$ and $M_w=\left(\frac{\lambda}{\gamma}\right)g'(0)x$ where $x=\frac{\bar{x}}{L}$. The non-dimensional rate of heat transfer, called the Nusselt number $Nu=\frac{Lq_w}{k\left(T_w-T_\infty\right)}$ and rate of mass transfer, called the Sherwood number $Sh=\frac{Lq_m}{D\left(C_w-C_\infty\right)}$ are given by $\frac{Nu}{\sqrt{\mathrm{Re}}}=\frac{1}{\theta(0)}$ and $\frac{Sh}{\sqrt{\mathrm{Re}}}=\frac{1}{\varphi(0)}$.

RESULTS AND DISCUSSION

The governing Equations (25) to (28) have been solved numerically using the Keller-box method [19]. This method has a second - order accuracy, unconditionally stable and is easy to be programmed. The calculations are repeated until some convergent criterion is satisfied and the calculations are stopped when $\delta f''(0)\le 10^{-8}$, $\delta g'(0)\le 10^{-8}$, $\delta\theta'(0)\le 10^{-8}$ and $\delta\varphi'(0)\le 10^{-8}$. In the present study, the boundary conditions for η at ∞ are replaced by a sufficiently large value of η where the velocity approaches 1, whereas the temperature and concentration approach zero. In order to see the effects of step size ($\Delta\eta$) we ran the code for our model with three different step sizes as $\Delta\eta$ = 0.001, $\Delta\eta$ = 0.01 and $\Delta\eta$ = 0.05 and in each case we found very good agreement between them on different profiles. After some trials we imposed a maximal value of η at ∞ as 6 and a grid size of $\Delta\eta$ as 0.01. In order to study the effects of the coupling number *N*, magnetic field parameter *M*, Prandtl number *Pr*, Schmidt number *Sc*, Dufour number D_f and Soret number S_r on the physical quantities of the flow, the remaining parameters are fixed as *B* = 1, λ = 1, Pr =0.7, Sc=0.2 and ϑ = 0.1.

In the absence of coupling number *N*, Magnetic parameter *M*, Soret number S_r, Dufour number D_f and buoyancy parameter *B* with R_i = 1, λ = 1, ϑ = 0, and *Sc* = 0.2 the results of non-dimensional skin-friction $f''(0)$ and Nusselt number *Nu* have been compared with the values of Ramachandran et al. [20], and it was found that they are in good agreement, as shown in table 1.

Fig. 2 depict that the variation of coupling number (*N*) on the profiles of non-dimensional velocity, microrotation, temperature and concentration with similarity variable η. The coupling number *N* characterizes the coupling of linear and rotational motion arising from the micromotion of the fluid molecules. Hence, *N* signifies the coupling between the Newtonian and rotational viscosities. As $N\to 1$, the effect of microstructure becomes significant, whereas with a small value of *N* the individuality of the substructure is much less pronounced. As $\kappa\to 0$ i.e. $N\to 0$, the micropolarity is lost and the fluid behaves as nonpolar fluid. Hence, $N\to 0$ corresponds to viscous fluid. It is observed from Fig. 2 that the velocity decreases with the increase of *N*. The maximum of velocity decreases in amplitude and the location of the maximum velocity moves farther away from the wall with an increase of *N*. The velocity in case of micropolar fluid is less than that in the viscous fluid case. It is seen from Fig. 3 that the microrotation component decreases near the vertical plate and increases far away from the plate with increasing coupling number *N*. The microrotation tends to zero as $N\to 0$ as is expected. It is noticed from Fig. 4 that the temperature increases with increasing values of coupling number. It is clear from Fig. 5 that the non-dimensional concentration increases from Newtonian case to non-Newtonian case.

The non-dimensional velocity, microrotation, temperature and concentration profiles, for different values of magnetic parameter *M* is illustrated from Figs. 6 - 9. It is observed from Fig. 6 that momentum boundary layer thickness decrease i.e., velocity increase as the magnetic parameter (*M*) increases. From Eq. (2) when $U_\infty(\bar{x})\ge\bar{u}$ (i.e. imposed pressure force dominates Lorentz force imposed by a transverse magnetic field normal to the flow direction, the effect of the magnetic interaction parameter is to increase the velocity. Similarly, $U_\infty(\bar{x})\le\bar{u}$, the effect of the magnetic interaction parameter is to decrease the velocity. From Fig. 7, it is clear that the microrotation component increases near the plate and deceases far away from the plate for increasing values of *M*. It is noticed from Fig. 8 that the temperature decreases with increasing values of magnetic parameter. It is clear from Fig. 9 that the non-dimensional concentration decreases with increasing values of *M*. The magnetic field gives rise to a motive force to an electrically conducting fluid, this force makes the fluid experience acceleration by decreasing the friction between its layers and thus decreases its temperature and concentration.

Figures 10 to 13 depict that the effect of mixed convection parameter *Ri* on the profiles of non-dimensional velocity, microrotation, temperature and concentration. Fig. 10 explains that the dimensionless velocity rises as *Ri* increases. The higher value of *Ri* leads to the greater buoyancy effect in mixed convection flow, hence it accelerate the flow. The non-

dimensional velocity of the fluid is increasing from pure forced convection (as $Ri \rightarrow 0$) to pure free convection ($Ri > 1$). It is seen from Fig. 11, that the magnitude of the microrotation increases with an increase in mixed convection parameter *Ri*. From Fig. 12, it is observed that the non-dimensional temperature of the fluid flow is decreasing from pure forced convection case ($Ri_i \rightarrow 0$) to the pure free convection case ($Ri > 1$). It is clear from Fig. 13 that the non-dimensional concentration decrease as *Ri* increases.

The effect of Soret number S_r and Dufour number D_f on the non-dimensional velocity, microrotation, temperature and concentration is shown in Figures 14 to 17. It is observed from Figure 14 that the velocity decreases with the increase of Dufour number D_f (or decrease of Soret number Sr). It is noticed from Fig. 15 that the microrotation component decrease near the vertical plate and increase far away from the plate with increasing Dufour number (or decreasing of Soret number), showing a reverse rotation near the two boundaries. The reason is that the microrotation field in this region is dominated by a small number of particles spins that are generated by collisions with the boundary. It is clear from Figure 16 that the temperature of the fluid increases with the increase of Dufour number (or decrease of Soret number). Figure 17 explains that the non-dimensional concentration of the fluid decreasing with increase of Dufour number Df (or decrease of Soret number Sr).

Table 2 shows that the effects of the coupling number *N*, Soret number S_r and Dufour number D_f, mixed convection parameter R_i and the magnetic parameter *M* on the skin friction C_f, the dimensionless wall couple stress M_w, heat transfer rate (Nusselt number *Nu*) and mass transfer rate (Sherwood number *Sh*). It is seen from this table that the skin friction, the wall couple stress heat and mass transfer rates decrease with the increasing coupling number *N*. For increasing value of *N*, the effect of microstructure becomes significant; hence the wall couple stress decreases. It is clear that skin friction, Nusselt number and Sherwood number are increasing as mixed convection parameter *Ri* is increasing, where as the wall couple stress decrease. As explained earlier, increasing effect of convection cooling as a result of the great buoyancy effect for large *Ri*. The effect of magnetic parameter is to increase the skin friction coefficient, Nusselt number, Sherwood number and decrease the wall couple stress. Further, it is observed that the skin friction coefficient and Nusselt number are decreasing and that of wall couple stress and Sherwood number are decreasing with the increasing of Dufour number D_f (or with the decrease of Soret number S_r).

Table 1 Comparison of results for a vertical plate in viscous fluids without stratification case Ramachandran et al. [20] for $Ri = 1.0$

	$f''(0)$		Nu	
Pr	[13]	Present	[13]	Present
0.07	1.8339	1.833887	0.7776	0.777615
7	1.4037	1.403650	1.6912	1.691297

Table 2 Effect of N,Ri, M, and S_r, D_f on skin friction, wall couple stress, Heat and Mass Transfer rates.

N	Ri	M	D_f	S_r	- f''(0)	- g''(0)	1/θ(0)	1/ϕ(0)
0.0	0.5	1.0	0.03	2.0	2.1168	0.0000	0.6965	0.3991
0.3	0.5	1.0	0.03	2.0	1.7620	0.0291	0.6711	0.3876
0.6	0.5	1.0	0.03	2.0	1.3132	0.0886	0.6301	0.3683
0.9	0.5	1.0	0.03	2.0	0.5946	0.2848	0.5300	0.3185
0.5	0.0	1.0	0.03	2.0	1.1154	0.0555	0.5954	0.3500
0.5	0.5	1.0	0.03	2.0	1.4783	0.0627	0.6466	0.3761
0.5	1.0	1.0	0.03	2.0	1.7871	0.0686	0.6841	0.3956
0.5	1.5	1.0	0.03	2.0	2.0627	0.0735	0.7143	0.4114
0.5	0.5	0.0	0.03	2.0	1.3285	0.0613	0.6354	0.3716
0.5	0.5	1.0	0.03	2.0	1.5045	0.0633	0.6466	0.3761
0.5	0.5	2.0	0.03	2.0	1.6621	0.0649	0.6557	0.3798
0.5	0.5	3.0	0.03	2.0	1.8061	0.0663	0.6635	0.3829
0.5	0.5	1.0	0.03	2.0	1.5045	0.0633	0.7402	0.3700
0.5	0.5	1.0	0.06	1.0	1.4838	0.0628	0.7327	0.4050
0.5	0.5	1.0	0.12	0.5	1.4754	0.0626	0.7235	0.4253

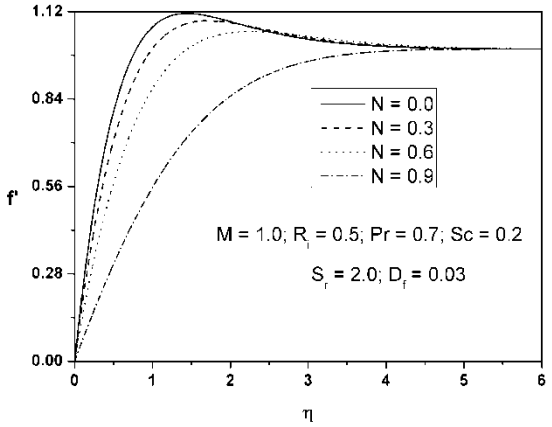

Figure 2 Profile for various values of coupling parameter *N*

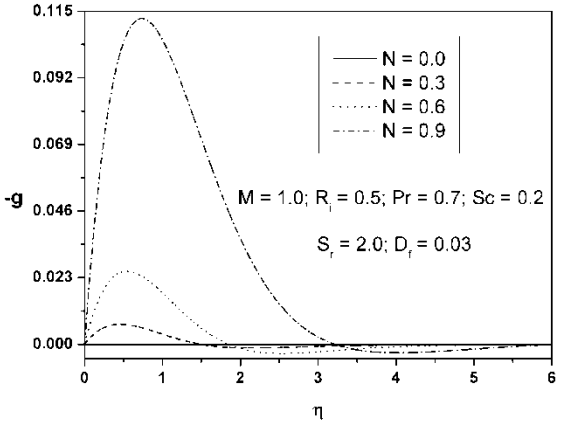

Figure 3 Microrotation Profile for various values of coupling parameter *N*

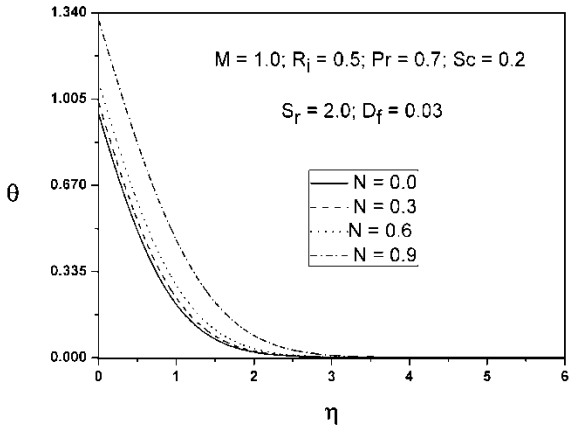

Figure 4 Temperature Profile for various values of coupling parameter *N*

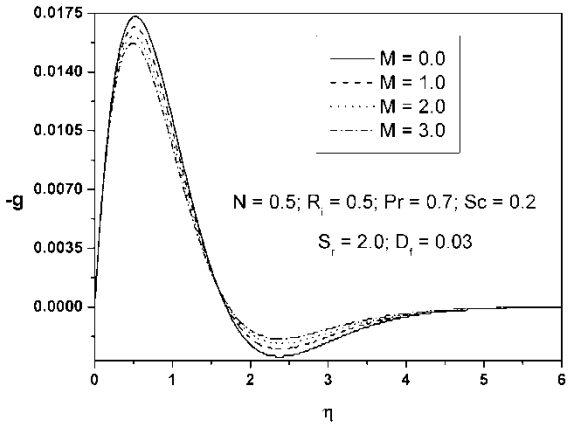

Figure 7 Microrotation Profile for various values of magnetic parameter *M*

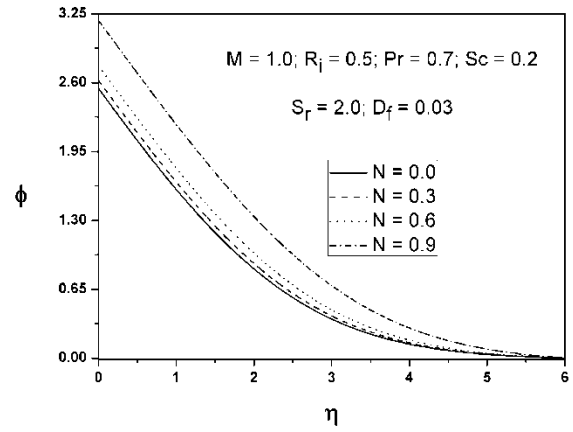

Figure 5 Concentration Profile for various values of coupling parameter *N*

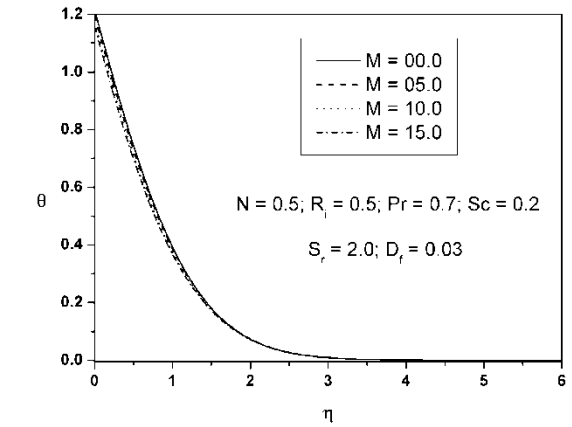

Figure 8 Temperature Profile for various values of magnetic parameter *M*

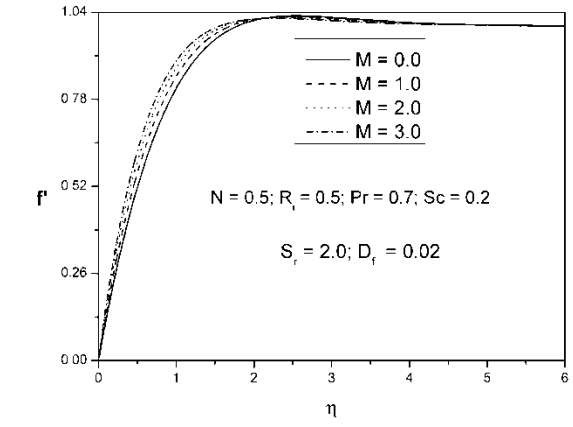

Figure 6 Velocity Profile for various values of magnetic parameter *M*

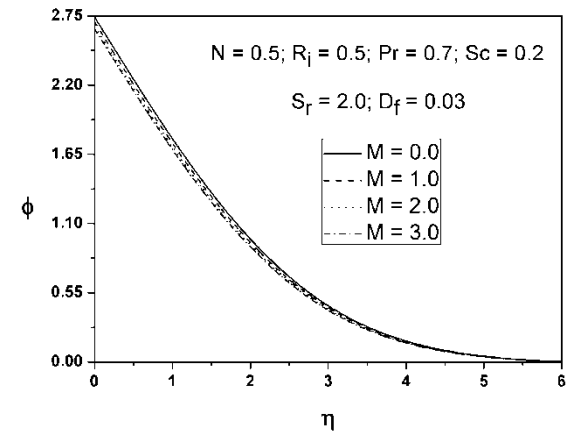

Figure 9 Concentration Profile for various values of magnetic parameter *M*

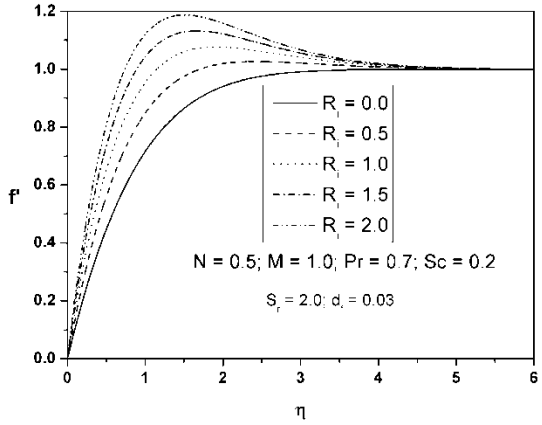

Figure 10 Velocity Profile for various values of mixed convection parameter *Ri*

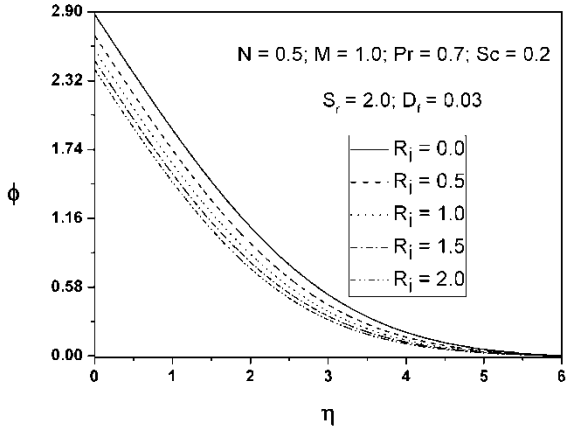

Figure 13 Concentration Profile for various values of mixed convection parameter *Ri*

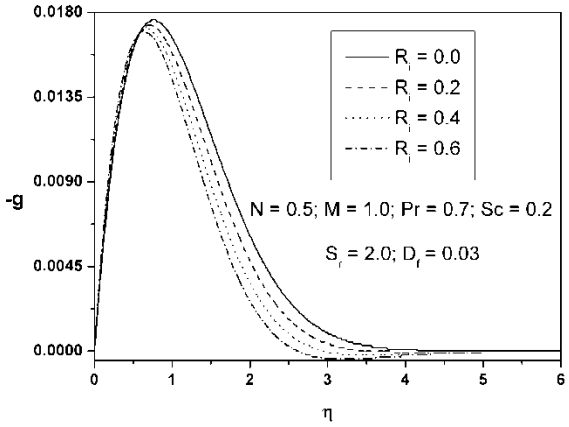

Figure 11 Microrotation Profile for various values of mixed convection parameter *Ri*

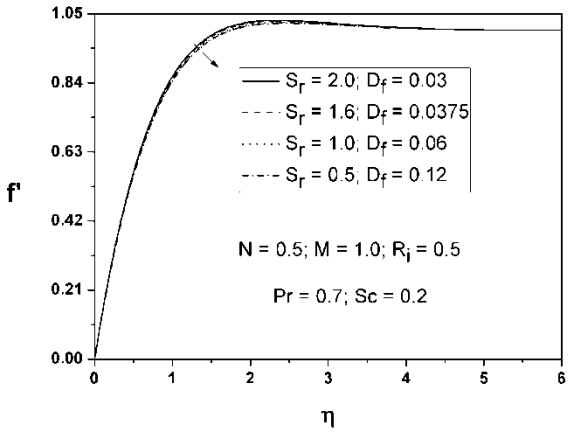

Figure 14 Velocity Profile for various values of Soret (S_r) and Dufour (D_f) numbers

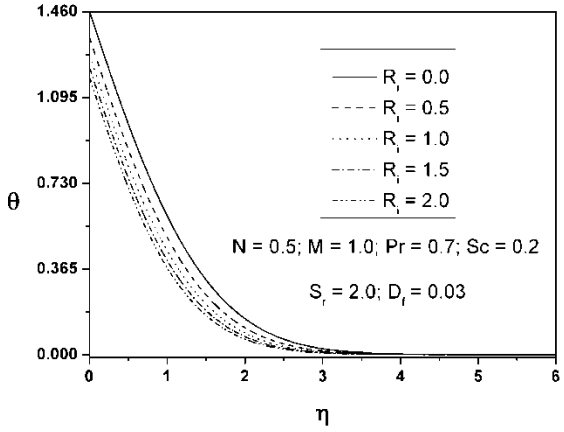

Figure 12 Temperature Profile for various values of mixed convection parameter *Ri*

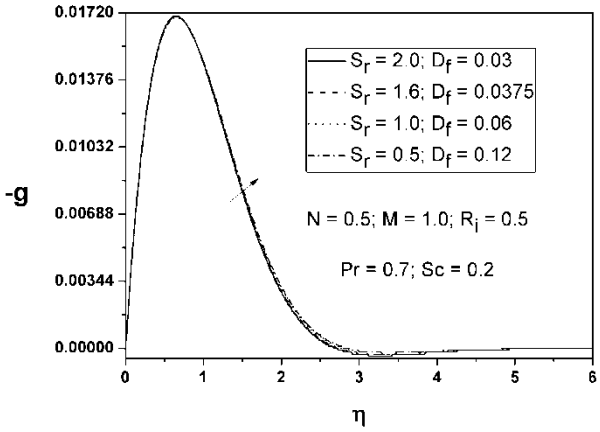

Figure 15 Microrotation Profile for various values of Soret (S_r) and Dufour (D_f) numbers

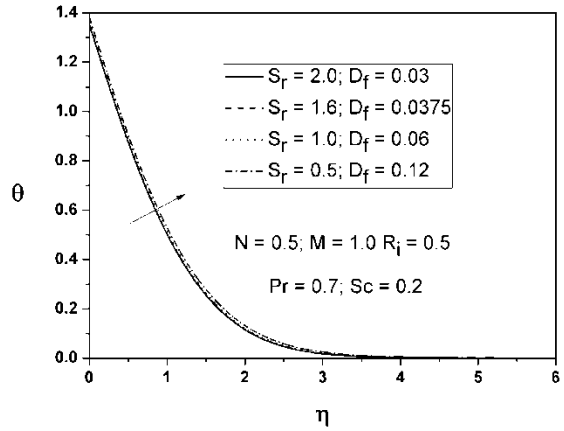

Figure 16 Temperature Profile for various values of Soret (S_r) and Dufour (D_f) numbers

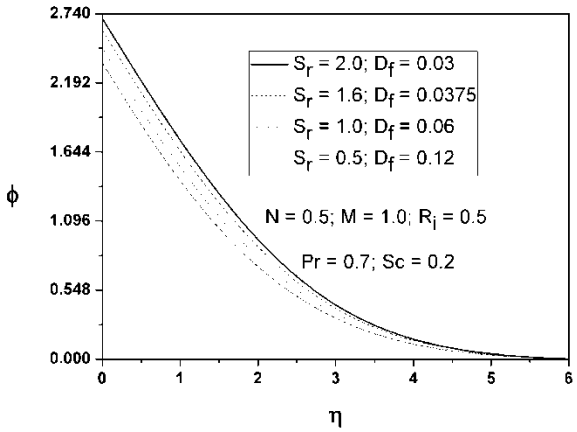

Figure 17 Concentration Profile for various values of Soret (S_r) and Dufour (D_f) numbers

CONCLUSION

- In this paper, a boundary layer analysis for mixed convection heat and mass transfer in an electrically conducting micropolar fluid over a vertical plate with variable heat and mass flux conditions in the presence of a uniform magnetic field, Soret and Dufour effects is considered. Numerical results indicates that the higher values of the coupling number N (i.e., the effect of microrotation becomes significant) result in lower skin friction, wall couple stress, and also the lower non-dimensional heat and mass transfer coefficients in the boundary layer compared to that of Newtonian fluid case ($N = 0$). As Ri increase the skin friction coefficient heat and mass transfer rates increases while the wall couple stress decreases. The increase in the magnetic parameter M increases the skin friction coefficient, wall couple stress, non-dimensional heat and mass transfer coefficients (Nu and Sh). The decrease in Soret number (S_r) (or increase in Dufour number D_f) results in lower skin friction and heat transfer rates and higher wall couple stress and mass transfer rates.

REFERENCES

[1] Eringen, A. C., Theory of Micropolar Fluids, *Journal of Mathematics and Mechanics,* Vol. 16, 1966, 1-18

[2] Seddeek, M. A., Odda, S. N., Akl, M. Y., and Abdelmeguid, M. S., Analytical Solution for the Effect of Radiation on Flow of a Magneto-Micropolar Fluid Past a Continuously Moving Plate With Suction and Blowing, *Computational Materials Science*, Vol. 46, 2009, 423-428

[3] Mahmoud, M., and Waheed, S., Effects of Slip and Heat Generation/Absorption on MHD Mixed Convection Flow of a Micropolar Fluid over a Heated Stretching Surface, *Mathematical Problems in Engineering*, Vol. 2010, 2010, 20

[4] Tzirtzilakis, E. E., Kafoussias, N. G., and Raptis, A., Numerical Study of Forced and Free Convective Boundary Layer Flow of a Magnetic Fluid over a Plate under the action of a Localized Magnetic Field, *Zeitschrift fur Angewandte Mathematik und Physik (ZAMP)*, Vol. 61, 2010, 929-947

[5] Hayat, T., Mixed Convection Flow of a Micropolar Fluid with Radiation and Chemical Reaction, *International Journal for Numerical Methods in Fluids*, Vol. 67, 2011, 1418-1436

[6] Das, K., Slip Effects on MHD Mixed Convection Stagnation Point Flow of a Micropolar Fluid towards a Shrinking Vertical Sheet, *Computers and Mathematics with Applications*, Vol. 63, 2012, 255-267

[7] Eckert, E. R. G., and Drake, R. M., *Analysis of Heat and Mass Transfer*, 1972, McGraw Hill

[8] Alam, M. S., and Rahman, M. M., Dufour and Soret Effects on Mixed Convection Flow Past a Vertical Porous Flat Plate with Variable Suction, *Nonlinear Analysis: Modelling and Control*, Vol. 11(1), 2006, 3-12

[9] Ali Chamkha, J., and Abdullatif Ben-Nakhi, MHD Mixed Convection Radiation interaction along a Permeable Surface immersed in a Porous Medium in the presence of Soret and Dufour Effects, *Heat and Mass Transfer*, Vol. 44, 2008, 845-856

[10] Rawat, M., and Bhargava, R., Finite Element Study of Natural Convection Heat and Mass Transfer in a Micropolar Fluid Saturated Porous Regime with Soret/Dufour Effects, *International Journal of Applied Mathematics and Fluid Mechanics,* Vol. 5, 2009, 58-71

[11] Srinivasacharya, D., and RamReddy, Ch., Effects of Soret and Dufour on Mixed Convection Heat and Mass Transfer in a micropolar fluid with heat and mass fluxes, *Journal of Heat Transfer*, Vol.133, 2010, 122502-1-7

[12] Hibiki, T., and Ishii, M., Development of one-group interfacial area transport equation in bubbly flow systems. *Int. J. Heat Mass Transfer.*, Vol. 45, 2002, 2351–2372.

[13] Tanthanuch, T., and Meleshko, S. V., On definition of an admitted lie group for functional differential equations, *Commun. Nonlinear Sci. Numer. Simul.*, Vol. 9, 2004, 117–125.

[14] Bluman, G., Broadbridge, P., King, J. R., and Ward, M. J., Similarity: generalizations, applications and open problems, *J. Eng. Math.,* Vol. 66, 2010, 1–9.

[15] Hamad, M. A. A., Analytical solution of natural convection flow of a nanofluid over a linearly stretching sheet in the presence of magnetic field. *Int. Commun. Heat Mass Transfer.*, Vol. 38, 2011, 487–492.

[16] Salama, F. A., Lie group analysis for thermophoretic and radiative augmentation of heat and mass transfer in a Brinkman-Darcy flow over a flat surface with heat generation, *Acta Mech. Sin.* Vol. 27(4), 2011, 531–540

[17] Rosmila A.B, Kandasamy R, Muhaimin I, Lie symmetry group transformation for MHD natural convection flow of nanofluid over linearly porous stretching sheet in presence of thermal stratification, *Appl. Math. Mech. -Engl. Ed.*, Vol. 33(5), 2012, 593–604

[18] N. Vishnu Ganesh et al., Lie symmetry group analysis of magnetic field effects on free convective flow of a nanofluid over a semi-infinite stretching sheet, *Journal of the Egyptian Mathematical Society* (2013), http://dx.doi.org/10.1016/ j.joems.2013.08.003
[19] Cebeci, T., and Bradshaw, P., *Physical and Computational Aspects of Convective Heat Transfer*, 1984, Springer Verlin
[20] Ramachandran, N., Chen, T. S., and Armaly, B. F., Mixed Convection in Stagnation Flows adjacent to Vertical Surfaces, *Journal of Heat Transfer*, Vol. 110, 1988, 373-377(OSTI ID: 5345718)